Supplementary Material

# Biodegradable pH-responsive amorphous calcium carbonate nanoparticle as an immunoadjuvant for multimodal imaging and enhanced photoimmunotherapy

Meng Wang [a], Benqing Zhou [a], Lu Wang [b], Feifan Zhou [a], Nataliya Smith [c], Debra Saunders [c], Rheal A. Towner [c], Jun Song * [a], Junle Qu * [a], and Wei R. Chen * [b]

[a] Key Laboratory of Optoelectronic Devices and Systems of Ministry of Education and Guangdong Province, College of Physics and Optoelectronic Engineering, Shenzhen University, Shenzhen 518060, P. R. China

[b] Stephenson School of Biomedical Engineering, University of Oklahoma, Norman, Oklahoma 73019, United States

[c] Advanced Magnetic Resonance Center, Oklahoma Medical Research Foundation, Oklahoma City, Oklahoma 73104, United States

**Keywords**: bioresponsive nanoparticle, amorphous calcium carbonate, cancer theranostic, phototherapy, immunotherapy

* Corresponding Author.
E-mail address: songjun@szu.edu.cn, jlqu@szu.edu.cn, and wchen@uco.edu

## Supplementary Figures

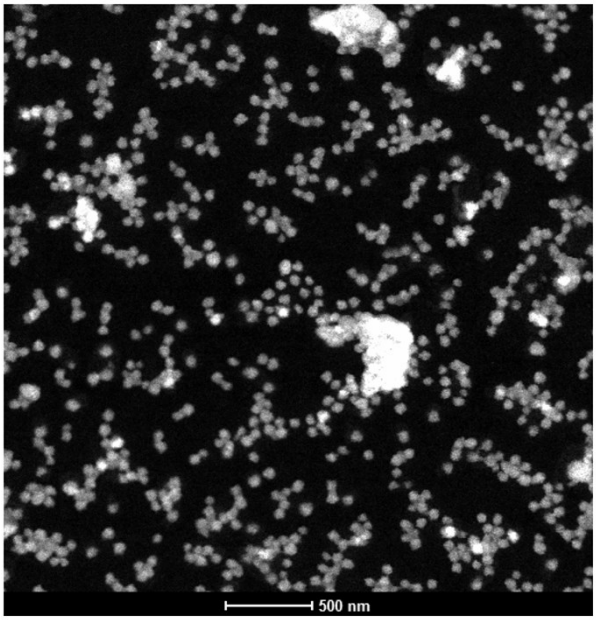


**Fig. S1** Transmission electron microscopy (TEM) image of ACC(Mn)-ICG nanoparticles (NPs). Scale bar = 500 nm.

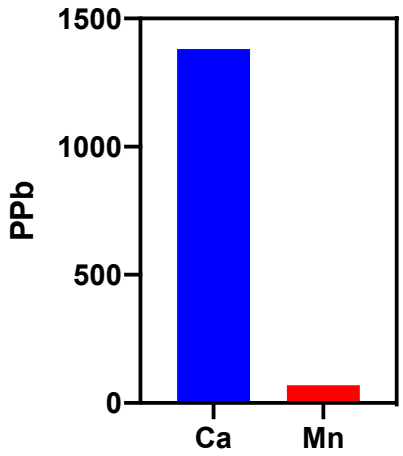


**Fig. S2** The contents of Ca and Mn elements in ACC(Mn)/ICG-PEG nanoparticles, which were analyzed via Inductive Coupled Plasma Emission Spectrometer (ICP). The result show that the doping concentration of Mn ions in ACC(Mn)-ICG NPs is ~5% (mol/mol).

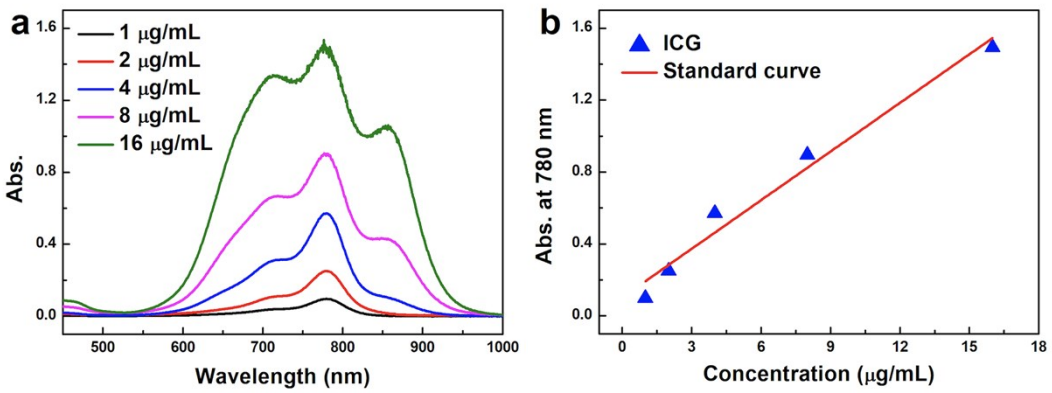


**Fig. S3** Quantitative analysis of indocyanine green (ICG) loaded in ACC(Mn)-ICG/PEG NPs. a) Absorption spectra of ICG solution. b) The standard curve of absorption for ICG.

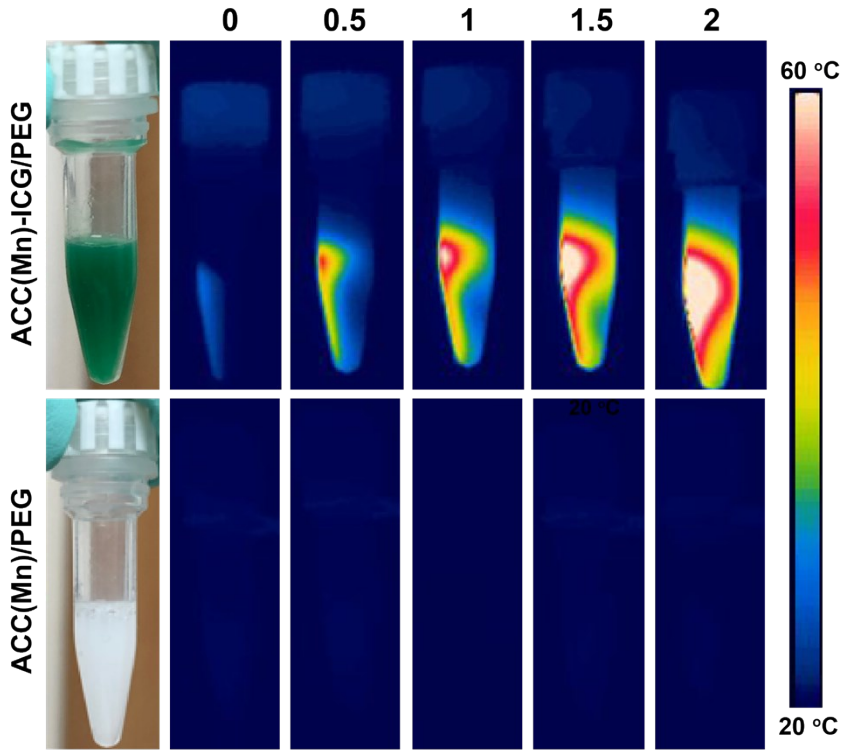


**Fig. S4** Infrared (IR) thermal images of ACC NPs and ACC(Mn)-ICG/PEG solutions upon an 805 nm laser irradiation (0.75 W $cm^{-2}$ for 2 min).

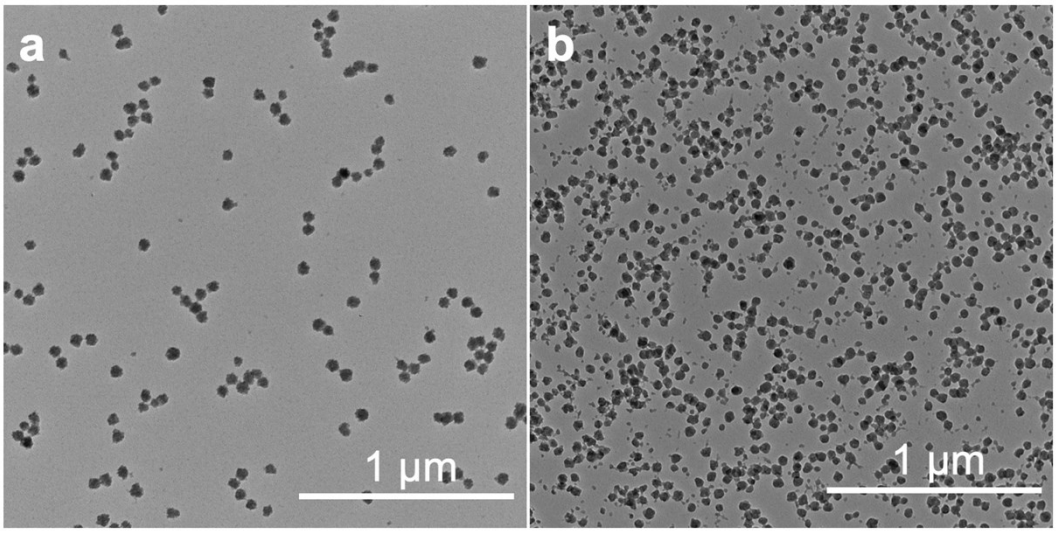


**Fig. S5** Representative TEM images of ACC(Mn)-ICG/PEG NPs after being immersed in pH 7.4 PBS buffer a) and 20% FBS solution b) for 24 h, respectively. Scale bar = 1 μm.

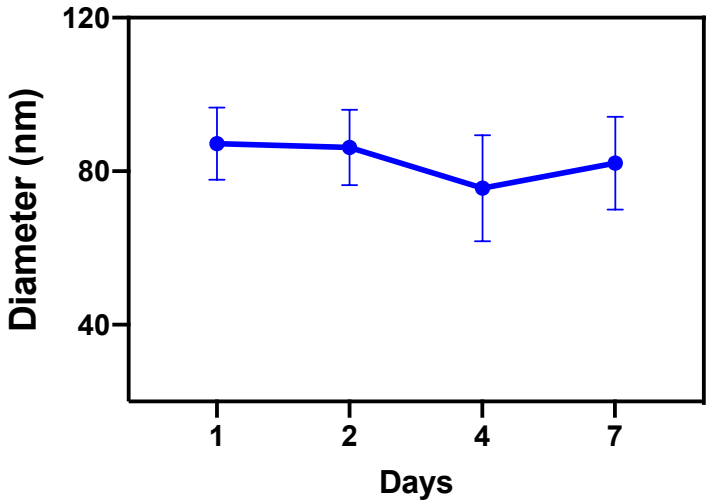


**Fig. S6** Hydrodynamic diameter distribution of ACC(Mn)/ICG-PEG NPs after being immersed in serum at different time point.

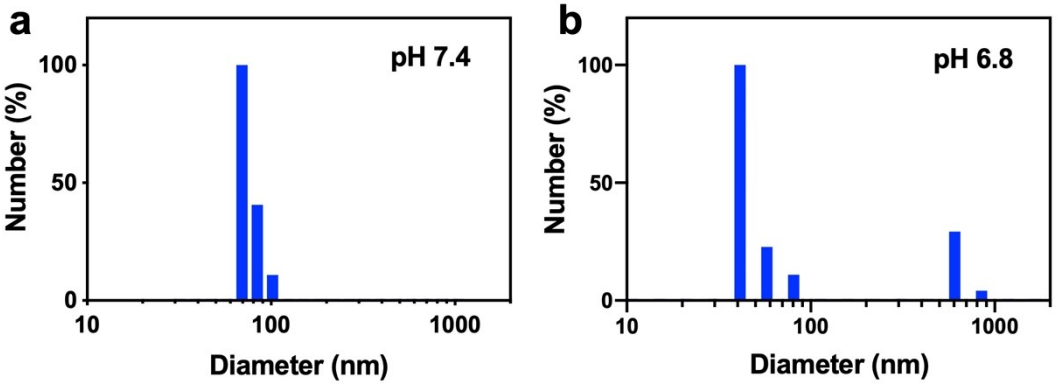


**Fig. S7** Hydrodynamic sizes of ACC(Mn)-ICG/PEG NPs after being immersed in pH 7.4 PBS buffer a) and pH 6.8 PBS buffer b) for 24 h, respectively.

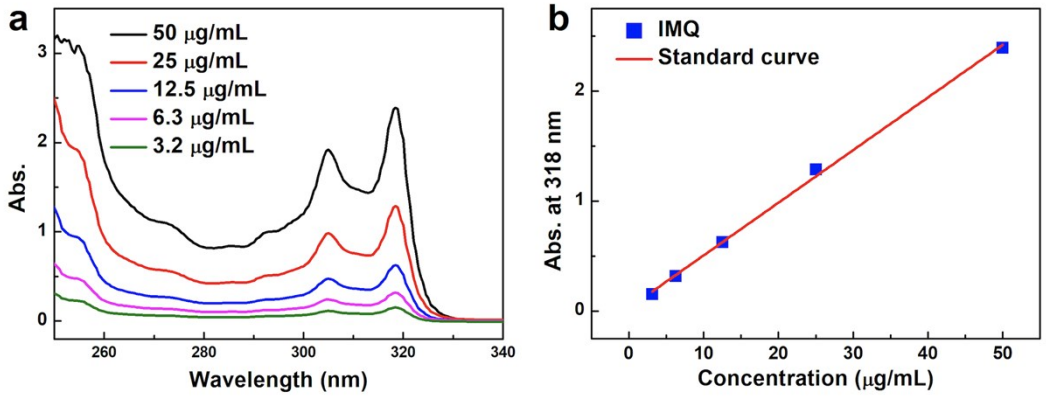


**Fig. S8** Quantitative analysis of imiquimod (IMQ) loaded in ACC(Mn)-ICG/PEG NPs. a) Absorption spectra of IMQ solution. b) The standard curve of absorption for IMQ.

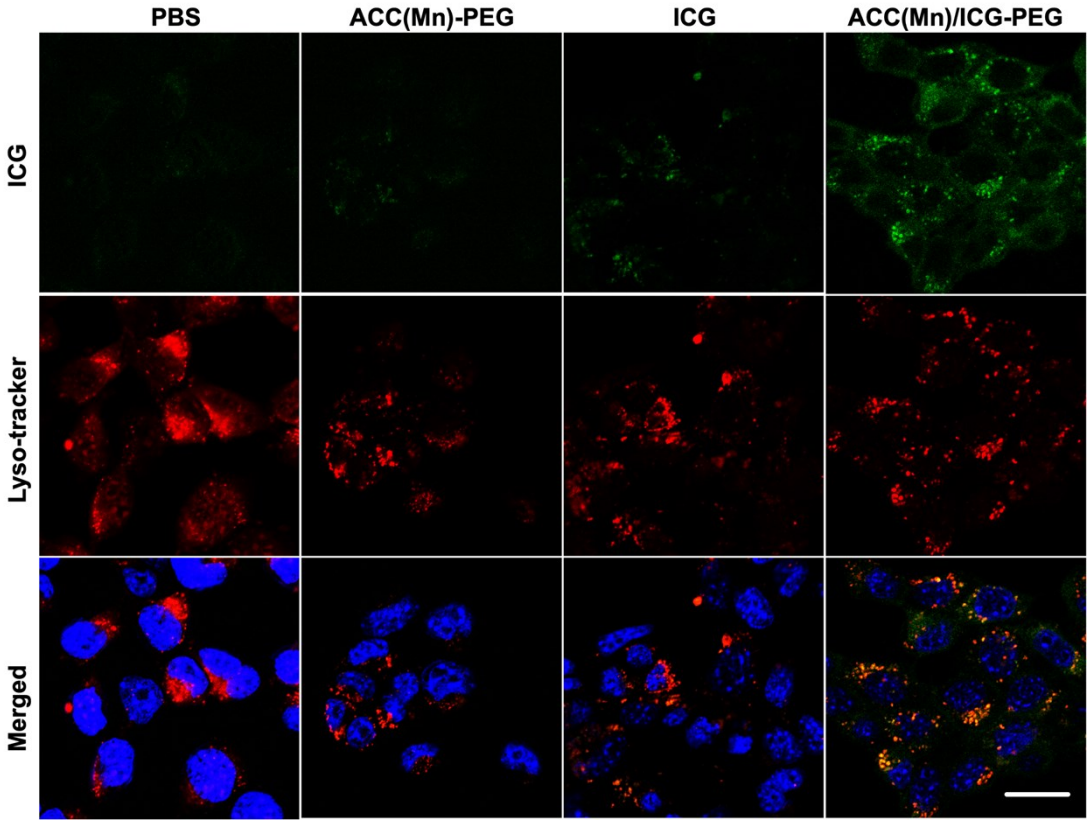


**Fig. S9** Representative fluorescence images of 4T1 cells after 4 h incubation with ACC(Mn)-PEG (200 μg $mL^{-1}$), ICG (20 μg $mL^{-1}$), and ACC(Mn)/ICG-PEG (200 μg $mL^{-1}$). Green: ICG, Red: Lyso-tracker, Blue: DAPI. (Scale bar = 20 μm)

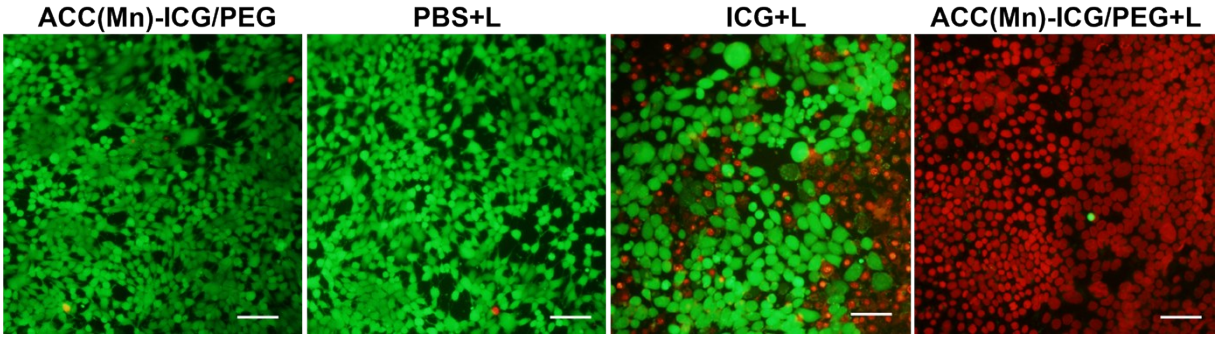


**Fig. S10** Fluorescence images of 4T1 cells after treated with ACC(Mn)-ICG/PEG, PBS + laser, ICG + laser, or ACC(Mn)-ICG/PEG + laser (805 nm, 0.75 W $cm^{-2}$ for 5 min). The cells were constained by calcein AM (Green, live cells) and propidium iodide (Red, dead cells) before imaging. Scale bar = 100 μm.

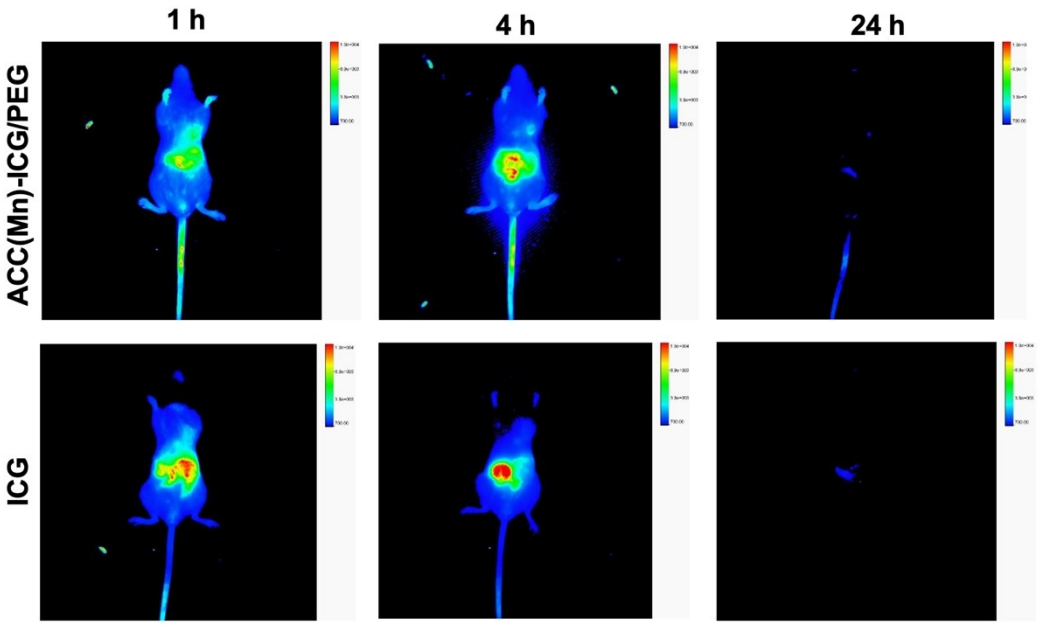


**Fig. S11** Representative *in vivo* fluorescence images of 4T1 tumor-bearing mice at indicated time points (1, 4, and 24 h) after intravenous injection of ICG (40 μg $mL^{-1}$, 100 μL) and ACC(Mn)-ICG/PEG NPs (10 mg $mL^{-1}$, 100 μL).

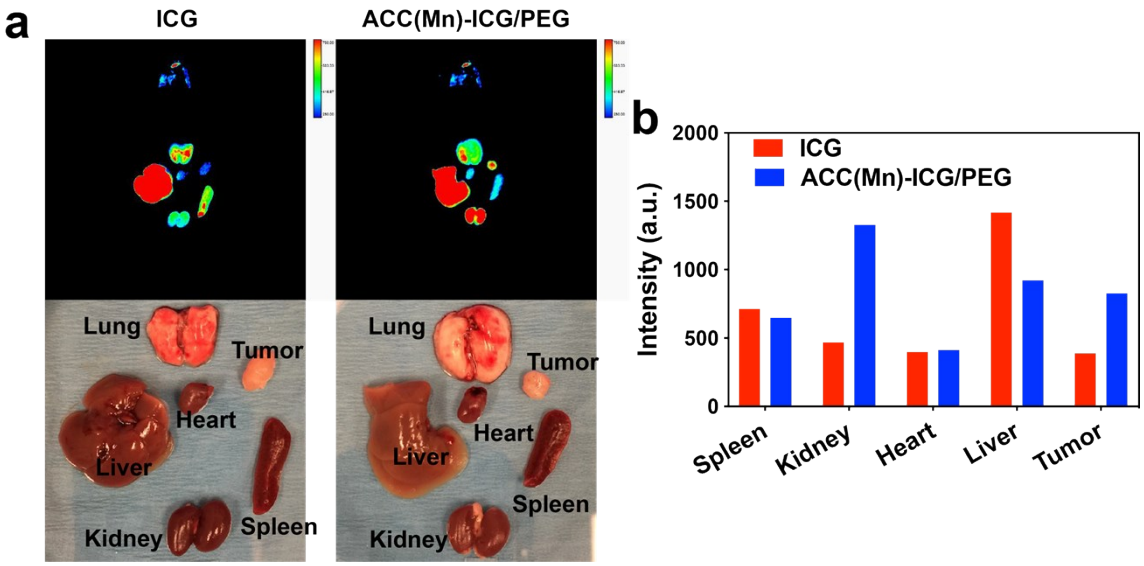


**Fig. S12** a) *Ex vivo* fluorescence images from excised organs and tumors at 7 h post injection of ICG and ACC(Mn)-ICG/PEG NPs. b) The semiquantitative analyses of fluorescence signals captured from these organs and tumors.

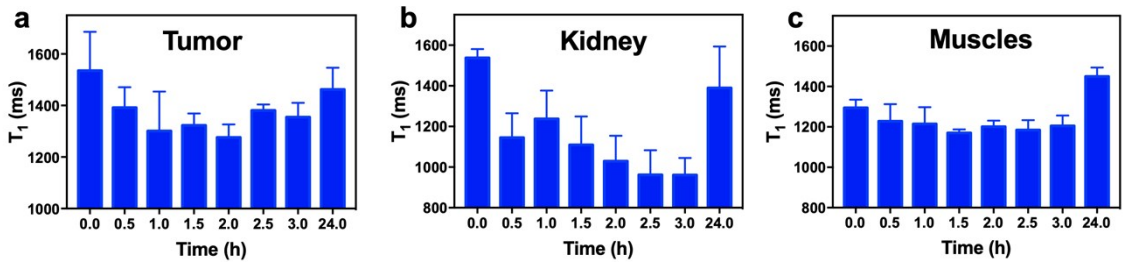


**Fig. S13** Corresponding representative $T_1$-weighted signals of tumor a), kidney b), and muscles c) at different time points after intravenous injection of ACC(Mn)-ICG/PEG.

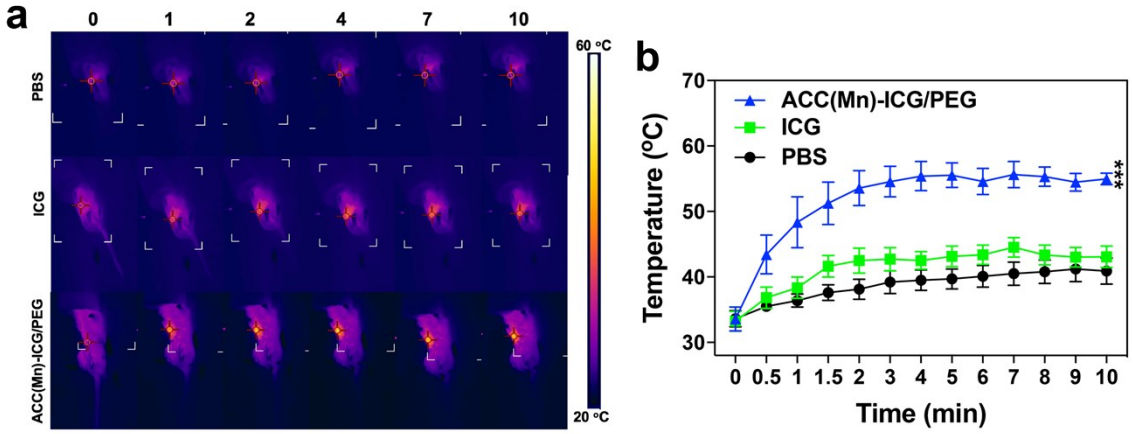


**Fig. S14** a) IR thermal images of 4T1 tumor-bearing mice treated with PBS, ICG, or ACC(Mn)-ICG/PEG in response to an 805 nm laser irradiation (0.75 W $cm^{-1}$ for 10 min). b) The tumor temperature based on IR thermal imaging data in a) (***$p < 0.001$ vs PBS). Data are expressed as means ± SD (n = 6).

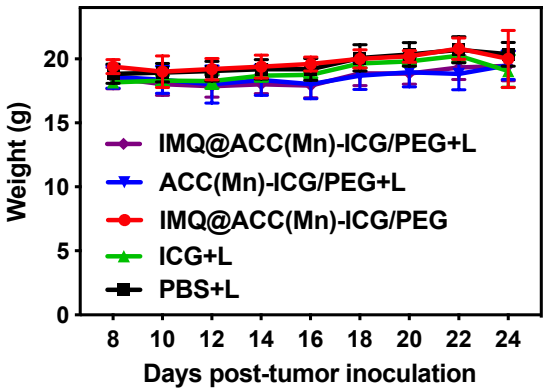


**Fig. S15** Average body weight of orthotopic 4T1 tumor-bearing mice of different groups. Data are expressed as means ± SD (n = 6).

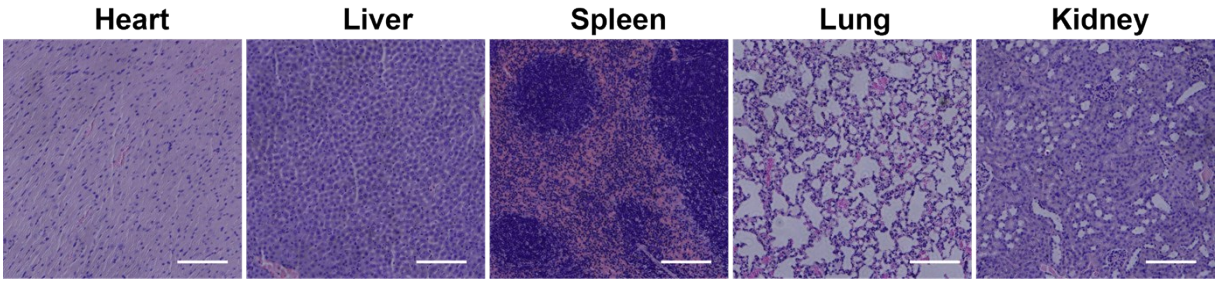


**Fig. S16** Representative H&E-stained images of major organs from the IMQ@ACC(Mn)-ICG/PEG + laser treated mice. Scale bar = 200 μm.

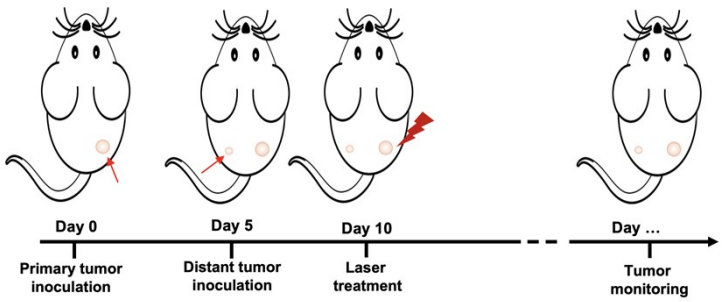


**Fig. S17** Schematic depiction of the experimental approach for the evaluation of the abscopal effect induced by ACC(Mn)-ICG/PEG based photoimmunotherapy.

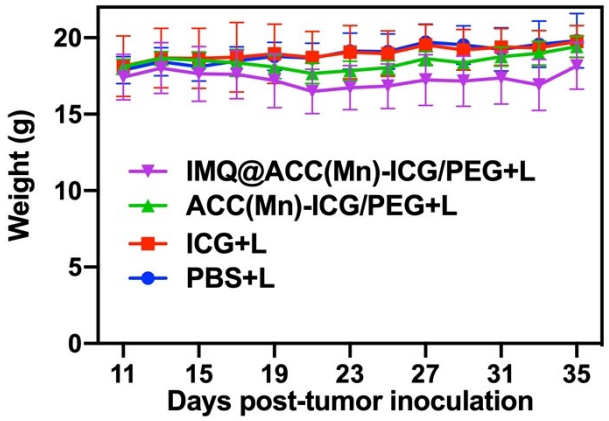


**Fig. S18** Average body weight of bilateral 4T1 tumor-bearing mice of different groups. Data are expressed as means ± SD (n = 5).

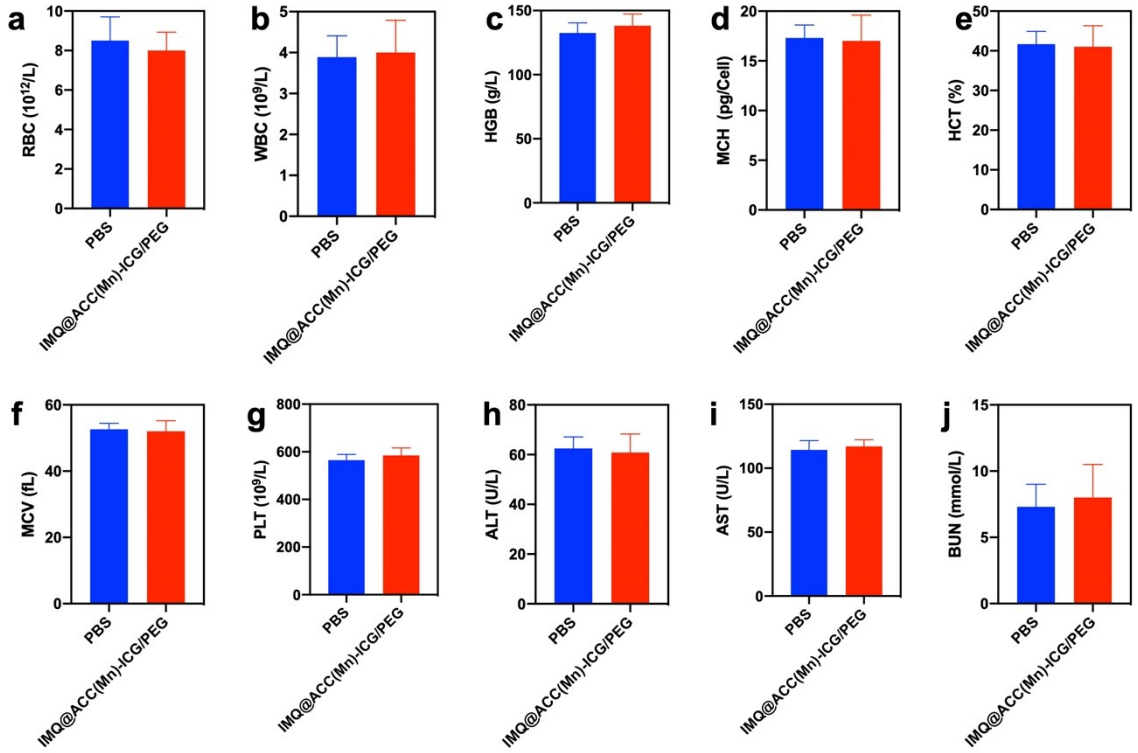


**Fig. S19** Hematology and blood biochemistry analysis of mice treated with IMQ@ACC(Mn)-ICG/PEG (20 mg $kg^{-1}$) at $30^{th}$ day for (a) Red blood cell (RBC) counts, (b) White blood cell (WBC) counts, (c) Hemoglobin (HGB), (d) Mean corpuscular hemoglobin (MCH), (e) Hematocrit (HCT), (f) Mean corpuscular volume (MCV), (g) Platelets (PLT), (h) Alanine aminotransferase (ALT), (i) Aspartate aminotransferase (AST), and (j) Blood urea nitrogen (BUN). Data are expressed as means ± SD (n = 5).

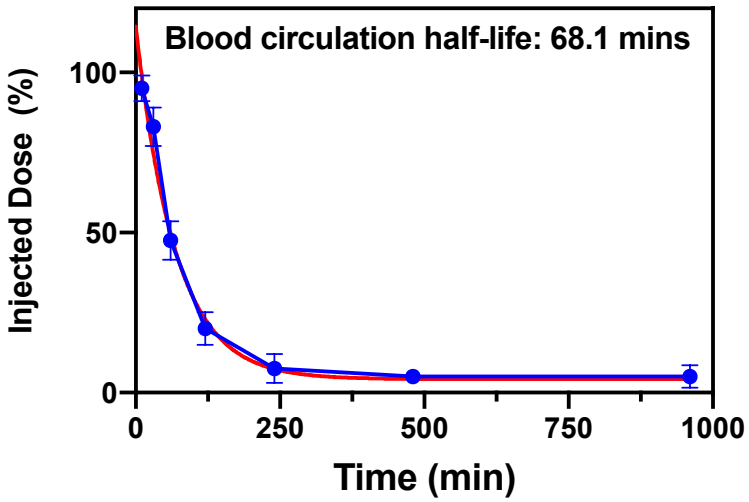


**Fig. S20** Pharmacokinetic property of IMQ@ACC(Mn)-ICG/PEG NPs were studied after intravenous injection to BALB/c mice (n = 3) at a dose of 40 mg/kg.

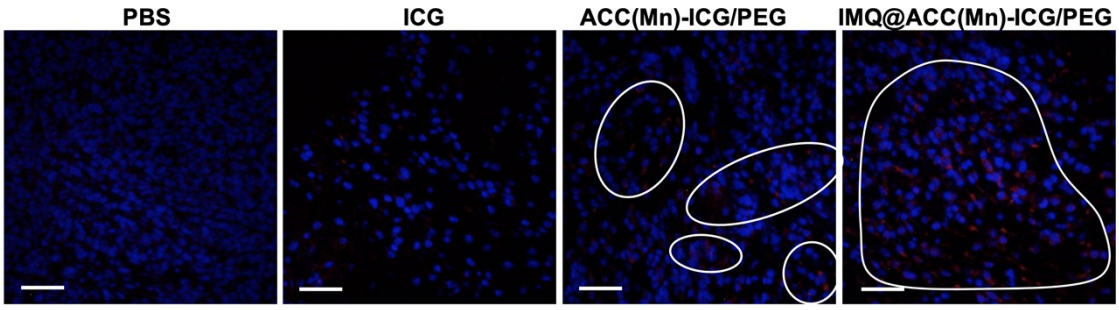


**Fig. S21** Representative images of tumors after staining of $CD11c^{+}$dendritic cells (Red) in primary tumors 1 day after the treatments. Scale bar = 200 μM.

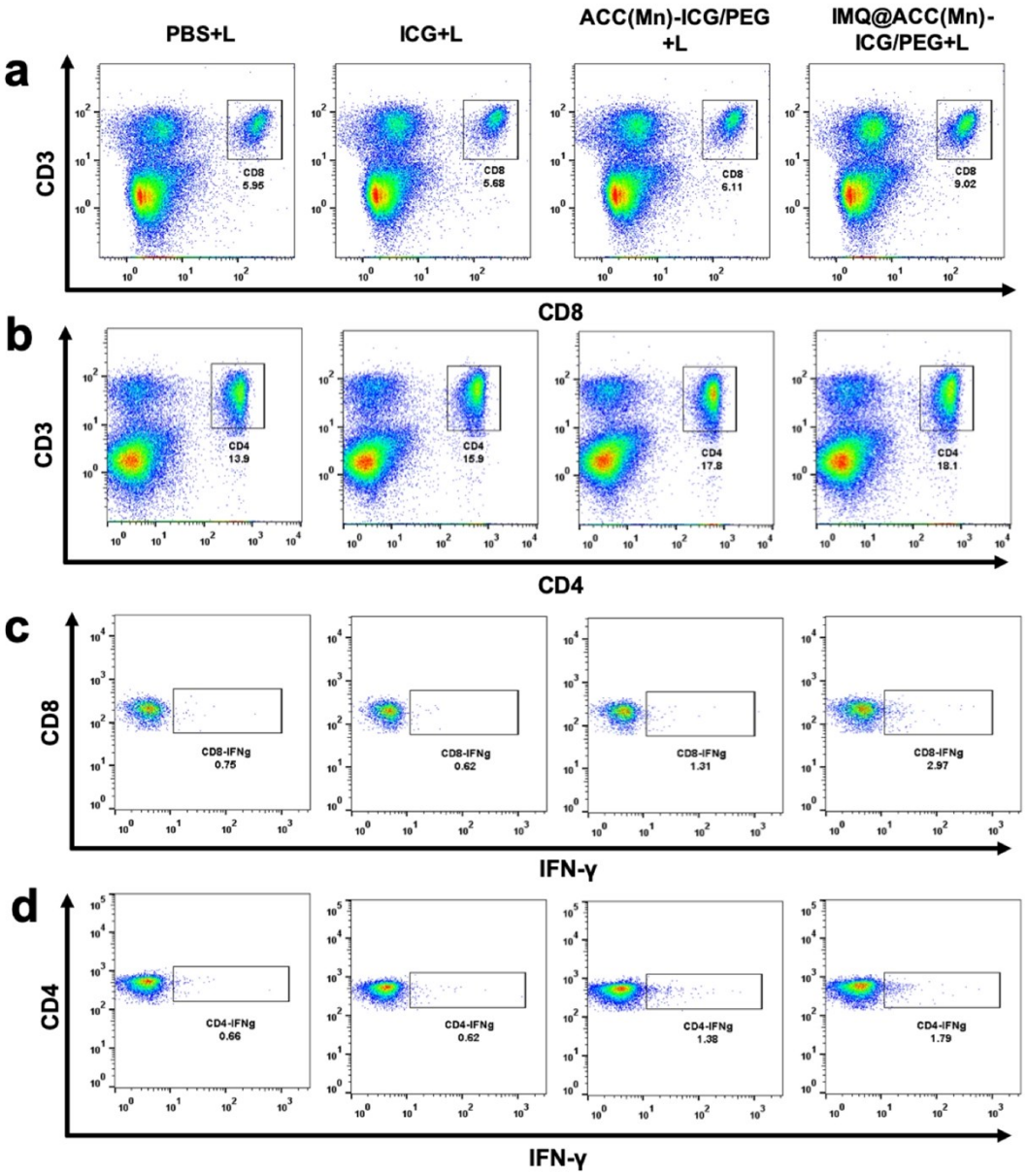


**Fig. S22** Representative flow plots used to quantify changes in the relative abundance of T cell subpopulations in splenocytes of mice by following different treatments.

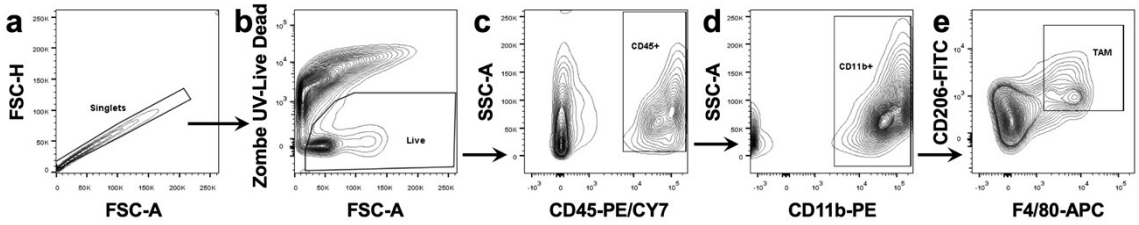


**Fig. S23** Gating strategy of TAM is performed based on the exclusion of doublets by FSC-A and FSC-H a), exclusion of dead cells b), selection of $CD45^+$ c), and further staining using CD11b d), F4/80 e) and CD206 e) with appropriate fluorescent dyes.

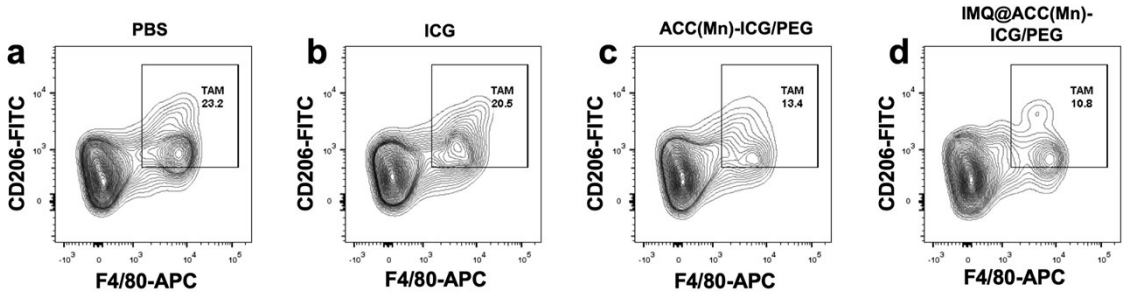


**Fig. S24** Representative flow plots used to quantify changes in the relative abundance of TAM cell subpopulations in tumors following different treatments.

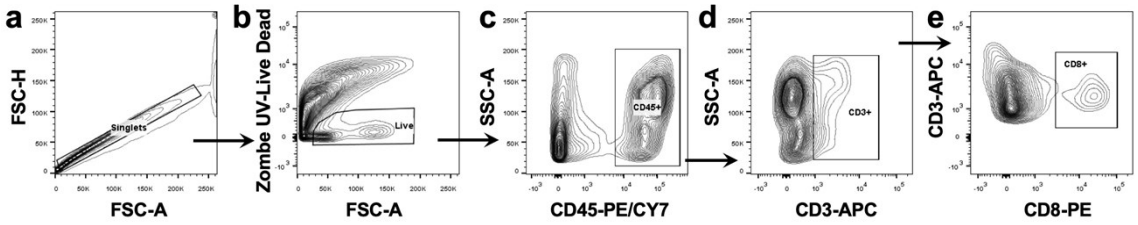


**Fig. S25** Gating strategy determine frequencies of T cells from distant tumors. The gating strategy was performed based on exclusion of doublets by FSC-A and FSC-H a), exclusion of dead cells b), selection of $CD45^+$ c), selection of $CD3^+$ d), and further staining using CD8 e) with appropriate fluorescent dyes to select $CD8^+$ T cells, respectively.

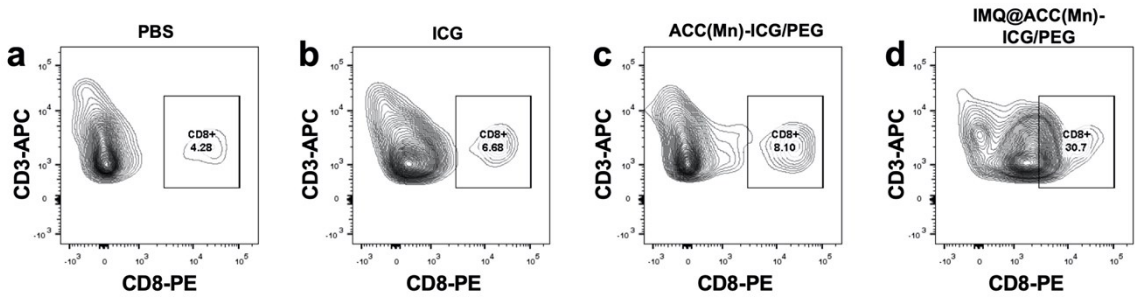


**Fig. S26** Representative flow plots used to quantify changes in the relative abundance of $CD8^+$ T cell subpopulations in unirradiated secondary tumors following different treatments of the primary tumors.

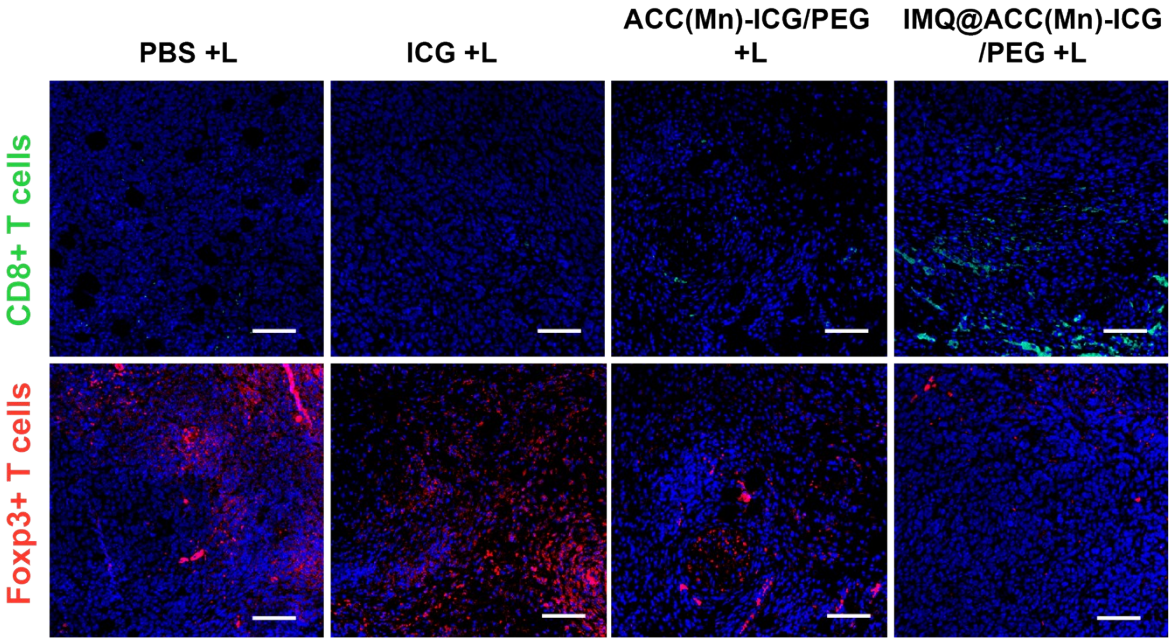


**Fig. S27** Representative images of tumors after staining of $CD8^+$ T cells (Green) and $Foxp3^+$ T cells (Red) in distant tumors 7 days after the treatments of the primary tumors. Scale bar = 200 μm.

## Experimental Section

### Characterization of ACC(Mn)-ICG NPs

Transmission electron microscopic (TEM) and element mapping were captured using a FEI Tecnai F20 TEM (USA) operating at an acceleration voltage of 200 kV. NIR-vis-NIR spectra were recorded on an absorption spectrometer (Cary 50 Bio, USA). The amounts of loaded ICG were quantitatively evaluated *via* UV–vis-NIR spectrophotometry (Cary 50 Bio). The ICG loading capacity was calculated using the following equation: loading efficiency of ICG (%) = ((weight of ICG) - (weight of unloaded ICG)) / (weight of ICG) × 100%. PL emission spectra were recorded on an Edinburgh Instruments FLS920 spectrometer (UK) under continuous (450 W) xenon lamp exposure at room temperature.

### Cell line and animals

The 4T1 cell line was obtained from the American Type Culture Collection (Rockville, USA), and this line was authenticated via morphology, karyotyping, and PCR-based approaches as well as tested for mycoplasma. 4T1 cells were cultured in RPMI 1640 (Gibco, USA) supplemented with 10% fetal bovine serum (FBS) (Gibco), 100 U $ml^{-1}$ penicillin, and 100 μg $mL^{-1}$ streptomycin (Gibco). Cell cultures were maintained below 50% confluence and early passage cultures (between four and nine) were utilized for the experiments. Female BALB/c mice (6 weeks, 18-20 g) were provided by Harlan Sprague Dawley Co. (USA). Mice were housed in the animal facility of the Department of Comparative Medicine at the University of Oklahoma Health Sciences Center (OUHSC, Oklahoma, USA). All experiments were conducted in compliance with the Guide for the Care and Use of Laboratory Animals published by the NIH and approved by the OUHSC Institutional Animal Care and Use Committee.

### PH-responsive release of IMQ

IMQ@ACC(Mn)-ICG/PEG NPs (2 mg) were diluted with 10 mL of PBS (pH 6.0, 6.8 or 7.4) and then incubated at 37 °C. At different time points, a 0.5 mL aliquot was withdrawn from each sample and centrifuged to collect the supernatant. The absorbance of the supernatant was recorded at 318 nm, and the amount of IMQ was quantitatively evaluated *via* UV–vis-NIR spectrophotometry (Cary 50 Bio).

### *In vitro* phototoxicity assay

Phototoxicity was analyzed by CCK-8 assay and Annexin V-FITC/PI Cell Apoptosis Kit assay

(eBioscience, USA). For CCK-8 assay, 4T1 cells were seeded into 96-well plates at a density of $5 \times 10^3$ cells per well and were cultured for 12 h. The cells were treated with ICG or ACC(Mn)-ICG/PEG NPs at various concentrations. After incubation for 4 h, cells were irradiated with an 805 nm laser for 5 min (0.75 W $cm^{-2}$) or kept in the dark, respectively. The cells were further incubated for 24 h and the cell viability was detected *via* CCK-8 assay, following the manufacturer's protocol. For the Annexin V-FITC/PI Cell Apoptosis Kit assay, 4T1 cells were seeded into 24-well plates ($5 \times 10^4$ cells/well) and cultured for 12 h. After treatment with PBS, ICG, and ACC(Mn)-ICG/PEG for a further 4 h, 4T1 cells were subjected to an 805 nm laser irradiation for 5 min (0.75 W $cm^{-2}$), followed by a further 24 h of incubation. Cell apoptosis was analyzed *via* flow cytometer (Becton Dickinson, San Jose, CA, USA).

**Intracellular ROS detection**

Intracellular ROS detection was analyzed by CLSM and flow cytometry using DCFH-DA as ROS sensor. For CLSM observation, 4T1 cells were seeded into 8-well chambered slides (Thermo Scientific, USA) at a density of $5 \times 10^3$ cells per well and were cultured for 12 h. After removal of the medium, cells were treated with PBS, ICG, and ACC(Mn)-ICG/PEG for a further 4 h and then irradiated with an 805 nm laser for 3 min (0.5 W $cm^{-2}$). The cells were further incubated with DCFH-DA (20 μM) for 30 min. Subsequently, the cells were observed via a TCS SP5 laser confocal microscope (TCS SP5II, Leica, Germany). For flow cytometry, 4T1 cells were seeded into 24-well plates ($5 \times 10^4$ cells/well) and cultured for 12 h. After treatment with PBS, ICG, and ACC(Mn)-ICG/PEG NPs for a further 4 h, 4T1 cells were subjected to 805 nm laser irradiation for 3 min (0.5 W $cm^{-2}$), followed by incubation with DCFH-DA (20 μM) for 30 min. ACC(Mn)-ICG/PEG NPs without laser irradiation served as dark control. Subsequently, the cells were harvested, and the fluorescence signals in response to ROS generation were analyzed via flow cytometer (Becton Dickinson, San Jose, CA, USA).

**Detection of ICD biomarkers**

CRT surface exposure was assessed via immunofluorescence assay and flow cytometry assay. For immunofluorescence analysis, 4T1 cells were seeded into 8-well chambered slides at a density of $8 \times 10^3$ cells per well and cultured for 12 h. The cells were incubated with PBS, ICG, or ACC(Mn)-ICG/PEG for 4 h and irradiated with an 805 nm laser for 5 min (at 0.75 W $cm^{-2}$). Cells treated with ACC(Mn)-ICG/PEG but without laser irradiation served as dark control. After a further 24 h of incubation, cells were washed twice with PBS and then incubated with anti-calreticulin antibody for 2 h at 4 °C. Subsequently, the cells were washed twice with PBS

and incubated with the Alexa Fluor 647-conjugated secondary antibody (BioLegend, USA) for 1 h. After staining with DAPI, the cells were analyzed via fluorescence microscopy (Olympus, Japan). For flow cytometric analysis, 4T1 cells were seeded into 24-well plates ($5 \times 10^4$ cells/well) and cultured for 12 h. The cells were treated with PBS, ICG, and ACC(Mn)-ICG/PEG NPs. After 4 h of incubation, cells were irradiated with an 805 nm laser for 5 min (0.75 W $cm^{-2}$). Cells treated with ACC(Mn)-ICG/PEG NPs without laser irradiation served as dark control. After a further 24 h of incubation, cells were collected, followed by incubation with anti-calreticulin antibody for 2 h. Subsequently, the cells were washed by PBS and incubated with Alexa Fluor 647-conjugated secondary antibody (BioLegend) for 1 h. Finally, the samples were analyzed via flow cytometry. Extracellular HMGB1 in conditioned media (serum-free) secreted from treated cells were measured via the HMGB1 ELISA Kit (R&D systems), following the manufacturer's instructions.

**Multimodal imaging**

BALB/c mice were subcutaneously injected with $5 \times 10^5$ 4T1 cells into the right breast pad. When tumor volumes reached ~150 $mm^3$, mice were randomly divided into two groups and either *i.v.* injected with ICG or with ACC(Mn)-ICG/PEG. After injection, the FL signals of ICG were recorded on the IVIS spectrum imaging system (Xenogen, USA) (ex: 780 nm) at 1, 4, and 24 h. The FL images of mice before injection served as blank control. For the biodistribution study, mice were sacrificed 24 h post injection, and both tumors and normal tissues were harvested and imaged. Similarly, for the MR imaging analysis, tumor-bearing mice were injected with ACC(Mn)-ICG/PEG via the tail vein. After injection, MR images of the tumor sites were recorded on a 7.1 Tesla MR scanner (Bruker Biospin, USA) at pre, 2, 3, and 24 h. The MR images of mice before injection served as blank control.

***In vivo* tumor models and treatment**

For the 4T1 orthotopic murine breast cancer model, BALB/c mice were subcutaneously injected with $5 \times 10^5$ 4T1 cells into the right breast pad. When tumors reached ~100 $cm^3$, mice were randomly assigned to their respective group and received PBS, ICG, ACC(Mn)-ICG/PEG, or IMQ@ACC(Mn)-ICG/PEG *i.v.* injections. Four hours after injection, mice were anaesthetized with 2% v/v isoflurane and the tumors were irradiated with an 805 nm laser for 10 min (at 1 W $cm^{-2}$). The tumor size was measured every two days, using digital caliper, and the tumor volume was estimated via ellipsoidal calculation as $V = (\text{width})^2 \times \text{length} \times \pi/6$. The mice were euthanized when tumors reached the maximum permitted size (2.0 cm in any dimension) or

when ulcerations occurred. For the distant tumor model, 5 days after $5 \times 10^5$ 4T1 were transplanted into the right flank of mice (primary tumor), a second tumor as the distant tumor ($5 \times 10^5$ 4T1) was inoculated into the left flank of each mouse. When primary tumors reached ~100 $cm^3$, mice were randomly assigned to their respective group and PBS, ICG, ACC(Mn)-ICG/PEG, or IMQ@ACC(Mn)-ICG/PEG was intratumorally injected into mice. Four hours after injection, mice were anaesthetized with 2% v/v isoflurane and primary tumors were irradiated with an 805 nm laser for 10 min (at 1 W $cm^{-2}$). The tumor size was measured every two days, using digital caliper, and the tumor volume was estimated *via* ellipsoidal calculation as $V = (\text{width})^2 \times \text{length} \times \pi/6$.

**Flow cytometry**

Tumors were harvested, treated with 1 mg $mL^{-1}$ collagenase I (Gibco, USA) for 30 min, and grounded using the rubber end of a syringe. Spleens were also harvested and grounded, and red blood cells were removed via ACK lysis buffer. Cells were filtered through nylon mesh filters and washed with PBS. The single-cell suspension was incubated with anti-CD16/32 (clone 93; Biolegend, USA) to reduce nonspecific binding to Fc receptors (FcRs). To analyze activated DCs, these were stained with anti-mouse CD11c-APC (Biolegend, USA) and anti-mouse CD86-PE (Biolegend, USA). To analyze M2-like TAMs, these were stained with Live/Dead-Zombe UV (Biolegend, USA), anti-mouse CD45-PE/CY7 (Biolegend, USA), CD11b-PE (Biolegend, USA), anti-mouse CD206-FITC (Biolegend, USA) and anti-mouse F4/80-APC (Biolegend, USA). To analyze the active T cells in tumors, the cells were stained with Live/Dead-Zombe UV (Biolegend, USA), anti-mouse CD45-PE/CY7 (Biolegend, USA), CD3-APC (Biolegend, USA) and anti-mouse CD8-PE (Biolegend, USA). To analyze active T cells in spleens, the cells were stained with anti-mouse CD3-APC CY7 (Biolegend, USA), anti-mouse CD4-APC (Biolegend, USA), and anti-mouse CD8a-PE (Biolegend, USA). For the analysis of IFN-γ production by T cells after stimulation ex vivo, the single-cell suspension was incubated with 4T1 lysates for 24 h. After stimulation, the cells were stained with anti-mouse CD3-APC CY7 (Biolegend, USA), anti-mouse CD4-APC (Biolegend, USA), anti-mouse CD8a-PE (Biolegend, USA), and anti-mouse IFN-γ-FITC (Biolegend, USA). The Stratedigm S1200Ex flow cytometer (Stratedigm, USA) was used for flow cytometry, and data analysis was conducted using FlowJo software (version 10.0.7).

**Cytokine detection**

Serum samples were isolated from mice after treatments and were diluted prior to analysis. Interleukin 6 (IL-6) and interleukin 12 (IL-12) were analyzed *via* ELISA kits (R&D Systems, USA) according to the manufacturer's protocol.

**Immunofluorescence assay**

Tumors were collected and frozen tissue sections of 6 mm thickness were prepared via cryostat. These sections were air-dried for at least 1 h and then fixed in acetone for 10 min at room temperature. After blocking with 20% donkey serum, the sections were incubated with antibodies, washed twice with PBS, and observed *via* fluorescence microscopy (Olympus, Japan).

**Statistical analysis**

Values are expressed as means ± standard error of the mean. The data was analyzed using GraphPad Prism software (Prism 5.0, GraphPad Software Inc., La Jolla, CA, USA). One-way analysis of variance (ANOVA) with Tukey's post hoc pairwise comparisons were employed to compare groups. A P value $< 0.05$ was considered statistically significant.